High-Resolution Mesoscale Analysis Data from the South China Heavy Rainfall Experiment (SCHeREX): Data Generation and Quality Evaluation*

NI Yunqi[1†](倪允琪), CUI Chunguang[2](崔春光), LI Hongli[2](李红莉), PENG Juxiang[2](彭菊香), QIU Xuexing[3](邱学兴), ZHANG Yanxia[4](张艳霞), XU Xiaolin[5](许晓林), GAO Mei[1](高 梅), JIE Lianshu[1](接连淑), and ZHANG Wenhua[1](张文华)

1 *Chinese Academy of Meteorological Sciences, China Meteorological Administration (CMA), Beijing* 100081

2 *Wuhan Institute of Heavy Rain, CMA, Wuhan* 430074

3 *Guangzhou Institute of Tropical and Marine Meteorology, CMA, Guangzhou* 510080

4 *Anhui Meteorological Observatory, Hefei* 230031

5 *Shanghai Typhoon Institute, CMA, Shanghai* 230030

(Received November 29, 2010; revised February 28, 2011)

ABSTRACT

In this study, the observational data acquired in the South China Heavy Rainfall Experiment (SCHeREX) from May to July 2008 and 2009 were integrated and assimilated with the US National Oceanic and Atmospheric Administration's (NOAA) Local Analysis and Prediction System (LAPS; information available online at http://laps.fsl.noaa.gov). A high-resolution mesoscale analysis dataset was then generated at a spatial resolution of 5 km and a temporal resolution of 3 h in four observational areas: South China, Central China, Jianghuai area, and Yangtze River Delta area. The quality of this dataset was evaluated as follows. First, the dataset was qualitatively compared with radar reflectivity and TBB image for specific heavy rainfall events so as to examine its capability in reproduction of mesoscale systems. The results show that the SCHeREX analysis dataset has a strong capability in capturing severe mesoscale convective systems. Second, the mean deviation and root mean square error of the SCHeREX mesoscale analysis fields were analyzed and compared with radiosonde data. The results reveal that the errors of geopotential height, temperature, relative humidity, and wind of the SCHeREX analysis were within the acceptable range of observation errors. In particular, the average error was 45 m for geopotential height between 700 and 925 hPa, 1.0–1.1°C for temperature, less than 20% for relative humidity, 1.5–2.0 m s^{-1} for wind speed, and 20°–25° for wind direction. The above results clearly indicate that the SCHeREX mesoscale analysis dataset is of high quality and sufficient reliability, and it is applicable to refined mesoscale weather studies.

Key words: diagnostic analysis, integration and assimilation, applicability, quality evaluation

Citation: Ni Yunqi, Cui Chunguang, Li Hongli, et al., 2011: High-resolution mesoscale analysis data from the South China Heavy Rainfall Experiment (SCHeREX): Data generation and quality evaluation. *Acta Meteor. Sinica*, **25**(4), 478–493, doi: 10.1007/s13351-011-0018-7.

1. Introduction

Heavy rainfall is one of the main disastrous weathers influencing China. The flood disaster induced by heavy rainfall inflicts increasing adverse impacts on social and economic development and national defense construction in China. Ni et al. (2006) pointed out that the major weather system inducing heavy rainfall is meso-β-scale heavy rainfall system with a spatial scale of 20–200 km and a temporal scale from a few hours to more than 10 h. New observational technology and dense observational networks and comprehen-

*Supported by the National Key Basic Research and Development (973) Program of China (2004CB418307), Special Public Welfare Research Fund for Meteorological Profession of Ministry of Science and Technology (GYHY200706012 and GYHY200906010), National Natural Science Foundation of China (40930951), Special Project of Scientific Research of Wuhan Institute of Heavy Rain (1011), and New Technology Promotion Project of China Meteorological Administration (CMATG2008Z08).

†Corresponding author: niyunqi@cams.cma.gov.cn.

(Chinese version published in Vol. 69, No. 1, 26–40, 2011)

©The Chinese Meteorological Society and Springer-Verlag Berlin Heidelberg 2011

sive observation experiments are required to resolve such a system, grasp features of heavy rainfall process, understand related physical mechanisms, obtain rational knowledge, and finally achieve accurate prediction of heavy rainfall (Tao, 1980). Investigations and studies on formative mechanism, prediction theories, and monitoring methods of heavy rainfall have always been an important research direction concerned by scientists as well as a major requirement for improving the capacity of disaster prevention and mitigation in China.

Since the 1960s, several field observation experiments of heavy rainfall have been conducted in China. In 1964, the heavy rainfall experiment in Yangtze River Delta was organized and carried out. During 1986–1990, "Studies on Monitoring and Nowcasting of Disastrous Weathers" was listed as a national key scientific and technological project. In 1997, "Study on Heavy Rainfall over Both Sides of Taiwan Straits and Its Periphery" was established as a Special Project of the National "Ninth Five-Year" Climbing Program (referred to as South China Heavy Rainfall Experiment–HUAMEX). In 2001/2002, a field experiment of heavy rainfall was performed in the middle and lower reaches of Yangtze River. Through these field experiments, large amounts of observational data were acquired for more profound understanding on the structure and mechanism of heavy rainfall. However, how to integrate and assimilate various observational data on different spatiotemporal scales has not been resolved in the past, and it is still difficult to give a complete structure of the meso-β-scale heavy rainfall system. Therefore, by using a data assimilation tool such as LAPS (Local Analysis and Prediction System; developed by the US National Oceanic and Atmospheric Administration (NOAA)), the observational data and weather dynamics could be combined in a consistent manner and high-resolution data can be generated to further reveal the evolutional mechanism and the structure and process of mesoscale heavy rainfall systems (Ni et al., 2006).

At present, the mesoscale observation system in China is fast approaching the advanced level in the world in terms of both instrumentation and observing strategy. The data observed by satellite, radar, microwave radiometer, GPS, wind profiler, and other unconventional means are increasingly sufficient and lead to a great improvement in data coverage and spatiotemporal resolution of data. This provides reliable sources for improving the analysis on mesoscale systems and the capacity of numerical forecast. Accordingly, mesoscale analysis and forecast techniques become the most active and new core technology in weather forecasting, providing increasingly strong support to short-term forecast and nowcast of disastrous weathers. Nonetheless, there are still great difficulties existing in the current forecast of mesoscale weather systems. The various observational data are independent to each other with no sufficient and ready-to-use mesoscale analysis data available, so it is hard for forecasters to take advantage of these data in their daily operations. This prohibits the forecasters' subjective initiatives. It is urgently required to integrate and assimilate these multi-channel data, and generate mesoscale analysis datasets with high spatiotemporal resolution as an intuitive tool for forecasters. In addition, the initial field of numerical models also requires more mesoscale information for better prediction accuracy. Therefore, development of a mesoscale analysis system is imperative.

The LAPS system, developed by the Earth System Research Laboratory (ESRL) of NOAA of US, was successfully transplanted by the Wuhan Institute of Heavy Rain of China Meteorological Administration. LAPS became a mesoscale analysis system, a component of the analysis and forecast platform for mesoscale disastrous weathers in the four experimental areas: South China, Central China, Jianghuai area, and Yangtze River Delta, during the South China Heavy Rainfall Experiment (SCHeREX). Although the LAPS system has been ported to run in China successfully with some analysis and test evaluation conducted on heavy rainfall processes (Cui et al., 2009; Li et al., 2009a), systematic tests and evaluations have not been carried out for a wide range of mesoscale analysis fields generated by large volumes of observational data from the field experiments. Accordingly, a mesoscale analysis dataset with high spatial and temporal resolutions was produced with LAPS for the SCHeREX in this study for systematic, comprehensive

and objective tests and evaluations, based on the observed data obtained during the intensive observation period in the above four experimental sites from May to July 2008 and 2009. The purpose of this study is to more rationally understand the quality of the SCHeREX mesoscale analysis data, its applicability to mesoscale analysis, and the capacity of the LAPS system, and to eventually provide users with a set of reliable and high-quality SCHeREX mesoscale analysis data.

2. Brief introduction of LAPS

LAPS is a mesoscale analysis and forecast system. The transplanting principle, structure and job processes of LAPS in China have been described in relevant papers (Li et al., 2008, 2009b). One most important function of LAPS is to combine and integrate multiple datasets acquired from various meteorological observation systems into a high-resolution gridded dataset over a particular area, thus generating a mesoscale analysis field. LAPS facilitates the integrated application of various sources of detected information, enhances spatial and temporal resolutions of data, improves cloud and precipitation descriptions, captures more detailed topography effect, and meets the requirement of the local weather analysis and forecast more flexibly. It is portable, scalable, convenient and efficient. The basic algorithm of the LAPS analysis system is to use distance weighted interpolation to acquire the data value at grid point based on the background field. Then, the relations among temperature, pressure, and wind as well as the vertical water vapor distribution are constrained by the three-dimensional and one-dimensional variations respectively (McGinley et al., 1991; Albers et al., 1996; Birkenheuer, 1999). Through adjusting distance weight and other parameters, the LAPS analysis system can make the analysis field very close to the observations.

The LAPS analysis system includes three parts: data integration module, data analysis module, and forecast model module. The function of data integration module in LAPS is to generate intermediate data on the LAPS grids through processing of various observational data and provide these data for data analysis module. Data analysis module includes the analyses of wind, temperature, height, cloud, and humidity. Many physical properties including the microphysics of precipitation/snowfall/liquid-equivalent, the quasi-geostrophic balance treatment of height and wind, cloud, soil moisture, etc., are derived by inversion. The output of LAPS includes not only conventional temperature, height, humidity, and wind fields, but also many guiding indexes, such as fire-inducing weather index, heat index, storm index, and three-dimensional freezing index. In addition, a variety of physical parameters such as surface potential temperature, surface wind field, sea level pressure, surface visibility, surface equivalent potential temperature, top height of boundary layer, and soil humidity are provided.

This system has been widely used in the US. The LAPS system provided services for the Summer Olympic Games in Atlanta (Snook, 1996; Snook et al., 1998). The water vapor analysis capacity of LAPS was improved through assimilation of GOES satellite radiation data and GPS vapor data (Birkenheuer, 1999, 2000). A comparison between LAPS output and the station observations was conducted by Hiemstra et al. (2006). It was pointed out that LAPS data described temperature and relative humidity fields accurately and had the strongest reproduction capability in wind field, but its accuracy decreased with the increase of altitude. McGlinley et al. (1991) disclosed that although most observational stations could not provide data at fine grid intervals, sufficient observation density could be achieved by adding radar and satellite data. Consequently, resolution of 10 km or even finer for observational data exists. In LAPS, all analyses contained an automatic quality control program; however, the apparatus and analytical errors would still cause a temperature error of about 1°C, a dew-point temperature error of 2°C (due to the lack of satellite data), a θ_{se} error of ±2°C, a wind velocity error of 1–2 m s^{-1}, a divergence error of 1×10^{-5} s^{-1}, a vertical velocity error of 2.5 cm s^{-1} at 4-km height (in the case of an average interval of 100 km between stations), and the vertical velocity error caused by topography was roughly estimated as 5–10 cm s^{-1}. Snook et al. (1998) deemed that in average view of LAPS surface analysis,

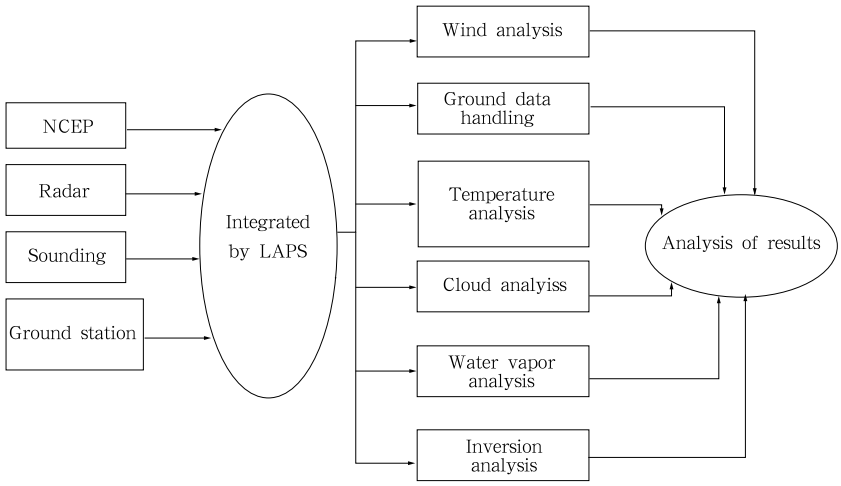

Fig. 1. Flow chart of LAPS used for the South China Heavy Rainfall Experiment (SCHeREX).

the difference of temperature between analysis and observation was 0.5–1.0 K; that of dew-point temperature analysis was 1.0–1.5 K; that of wind velocity was 1–2 m s^{-1}, and all differences were acceptable as with the instrumental error.

Through collaboration with US ESRL, Wuhan Institute of Heavy Rain introduced and debugged this system, modified data format, amended some parameters and source codes, and finally successfully ported this system into China. The SCHeREX was carried out in 12 provinces and two cities in South China from 1 May to 20 July of 2008 and 2009. The LAPS analysis system was used in SCHeREX for integration and assimilation of various conventional and unconventional data. In accordance with the LAPS job flow (Fig. 1), the SCHeREX mesoscale analysis dataset was created with a horizontal resolution of 5 km and a temporal resolution of 3 h in four observational sites, i.e., Central China, South China, Jianghuai area, and Yangtze River Delta. At present, the LAPS analysis system has been run for a two-year trial operation in Hubei, Anhui, Shanghai, Guangdong, and the Chinese Academy of Meteorological Sciences, and the generated mesoscale analysis data have been employed in the mesoscale analysis research and forecast services for the above observational areas.

3. SCHeREX mesoscale analysis

During the SCHeREX in May–July 2008 and 2009, four field observation areas (see Fig. 2) were chosen, and high-resolution mesoscale analysis data over these areas were generated by applying the LAPS system. The data integrated and analyzed by LAPS included surface observational data at conventional and automatic weather stations, four-time daily upper air sounding data during the intensive observation period, and SA- and SB-band Doppler radar data. The observational instruments are listed in Table 1. Comprehensive data from various sources were available. For example, the data over Central China included information from 13 radars, 12 radiosonde stations, and more than 1600 automatic weather stations and conventional surface observation stations (Fig. 2).

The above data in the four observational areas were integrated and assimilated by LAPS to generate the SCHeREX mesoscale analysis with a spatial resolution of 3 km and a temporal resolution of 3 h. In particular, mesoscale analysis data with a temporal resolution of 1 h were also generated in the Dabie Mountain of Jianghuai area. The SCHeREX mesoscale analysis had 21 vertical levels with the top pressure of 100 hPa. The meteorological variables included temperature, geopotential height, humidity, wind direction, and wind speed as well as various surface and near-surface meteorological variables. Valuable physical parameters such as CAPE index, K index, convective inhibition index CIN, and lifting index were also provided for diagnostic analysis of severe mesoscale convective weather.

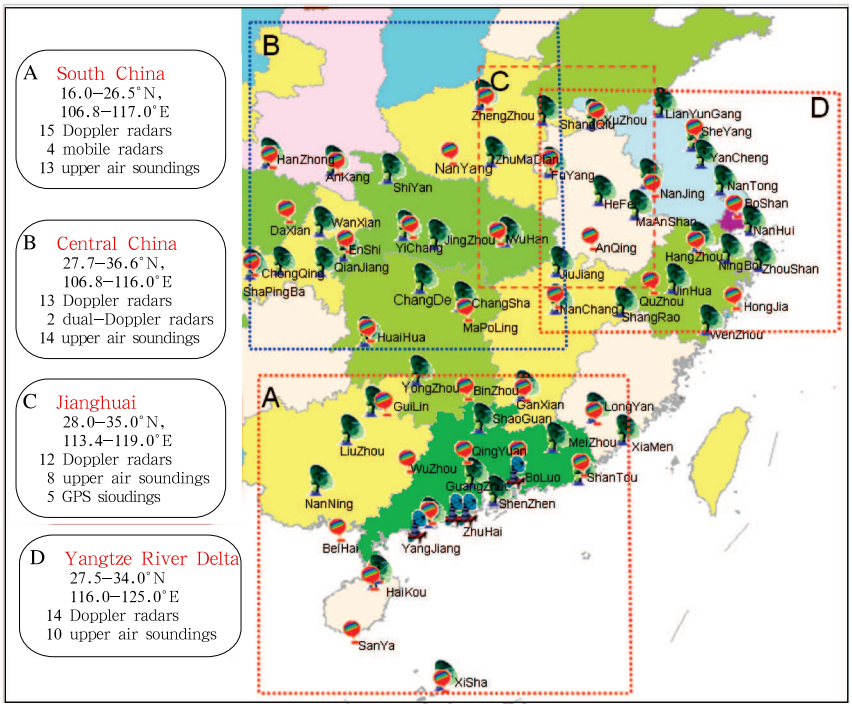

Fig. 2. The four observation areas and various types of observations in SCHeREX.

Table 1. Number of major instruments used in SCHeREX

	South China	Central China	Jianghuai	Yangtze River Delta	Total
Operational radars	16	13	13	14	56
Operational sounding stations	13	12	10	9	44
Added sounding stations			5		5
Mobile radars	2	1	1	1	5
Automatic stations	1700	1690	2100	1458	6948

4. Capability of SCHeREX mesoscale analysis in capturing mesoscale weather systems

The capability of SCHeREX mesoscale analysis in reproducing mesoscale systems (especially the meso-β-scale system) is assessed in this section. Whether the SCHeREX mesoscale analysis could reasonably capture the mesoscale systems inducing strong precipitation is the most important indicator of the performance of LAPS. The SCHeREX mesoscale analysis was first used to identify the mesoscale weather systems that had incurred heavy rainfall. Then, we analyze these weather systems in comparison with satellite and radar observations.

4.1 The heavy rainfall systems in the SCHeREX mesoscale analysis

The day with 24-h precipitation more than 50 mm observed at a single conventional observation station is defined as a heavy rainfall day. Statistics of heavy rainfall days was conducted over the four experimental areas from 1 May to 20 July 2008 and 2009, and the SCHeREX mesoscale analysis wind and height fields on these heavy rainfall days were analyzed. At 925, 850, and 700 hPa, the mesoscale systems (mainly the meso-β-scale system) on spatial scales of over several tens to 1–2 hundred kilometers were identified and their association with surface station observed heavy rainfall was examined. The results are shown in Table 2.

It can be seen from the statistical results that LAPS had a strong capability in reproduction of most meso-β-scale systems inducing heavy rainfall, especially for the cases of heavy rainfalls with wide range, concentrated location, consecutive occurrence and weak locality. In addition, different types of mesoscale systems dominated at different heights in

different regions, suggesting that certain differences might exist in the vertical structure of mesoscale systems in different areas. The mesoscale systems active in the South China pre-rainy season included convergence line at mid-low levels, shear line, and low-pressure vortex system such as the eastward moving Southwest China vortex. The weather system in the South China post-rainy season was mainly typhoon. The mesoscale systems influencing Central China, Jianghuai, and Yangtze River Delta mainly included shear line, convergence line, and low-pressure vortex. In addition, no weather system was found to be associated with concentrated extremely severe convective rainfall, rainfall with strong locality (little or no rain in the surrounding), and unevenly distributed rainfalls, among which some even occurred at only one single station (i.e., single-point storm precipitation). Such precipitation might be produced by small-scale (meso-γ-scale) systems with a short duration, and SCHeREX mesoscale analysis had a weak capacity in reproducing these small-scale convective systems.

Table 2. Statistics of heavy rainfall days and mesoscale systems from the SCHeREX analysis over the period of 1 May–20 July in both 2008 and 2009

Experimental area	Heavy rainfall days		Mesoscale systems
Jianghuai	33	700 hPa 24 (77%)	Convergence line (4), low-pressure vortex and trough (15), shear line (5)
		850 hPa 25 (78%)	Low-pressure vortex (12), convergence line (9), shear line (4)
		925 hPa 27 (80%)	Convergence line (15), low-pressure vortex (7), trough (3), shear line (2)
South China	49	37 (76%)	Convergence line, shear line, and vortex system
Central China	50	700 hPa 49 (98%)	Convergence line (8), low-pressure vortex (17), shear line (15), trough (6), mesoscale cyclone (3)
		850 hPa 46 (92%)	Convergence line (12), low-pressure vortex (15), shear line (10), trough (5), mesoscale cyclone (4)
		925 hPa 46 (92%)	Convergence line (20), low-pressure vortex (10), shear line (9), trough (2), mesoscale cyclone (5)
Yangtze River Delta	38	38 (100%)	Low-pressure vortex (7), convergence line (14), trough (3), shear line (8), meso-α-scale vortex (6)

4.2 Comparison between the SCHeREX mesoscale analysis and the observations

The heavy rainfall cases in South China on 18 May 2008, in Yangtze River Delta on 10 June 2008, in Jianghuai River basin on 21 June 2008, and in South China on 2 June 2009 were selected for the comparison. The development and evolution of the mesoscale systems in the SCHeREX mesoscale analysis were analyzed and compared with surface precipitation, radar echo and TBB.

From the SCHeREX mesoscale analysis, at 1800 UTC 18 May 2008, precipitation occurred in south Guangxi and an obvious mesoscale convective system formed and developed in the lower troposphere (Fig. 3). At 700 hPa, a mesoscale cyclone was generated in central southern Guangxi (with a horizontal range of about 200 km), and the radar echoes of severe convection were located in the warm and moist southwesterly airflow to the south of the cyclone; at 850 hPa, strong radar echoes existed corresponding to the meso-β-scale vortex in southern Guangxi and the mesoscale convergence line at 925 hPa. Subsequently, the whole mesoscale convective system gradually moved toward southeast. Three hours later, the meso-β-scale vortex at 850 hPa moved to the border of Guangdong and Guangxi provinces, accompanied by strong radar echoes. In this process, the duration of heavy rain cluster was consistent with the life span of the meso-β-scale cyclone and matched the actual radar echoes. This indicates that strong precipitation was induced by the eastward movement of the meso-β-scale cyclone in South China, and the development and evolution of the mesoscale convective system can be well reproduced by the SCHeREX mesoscale analysis.

A heavy rainfall event occurred in Yangtze River

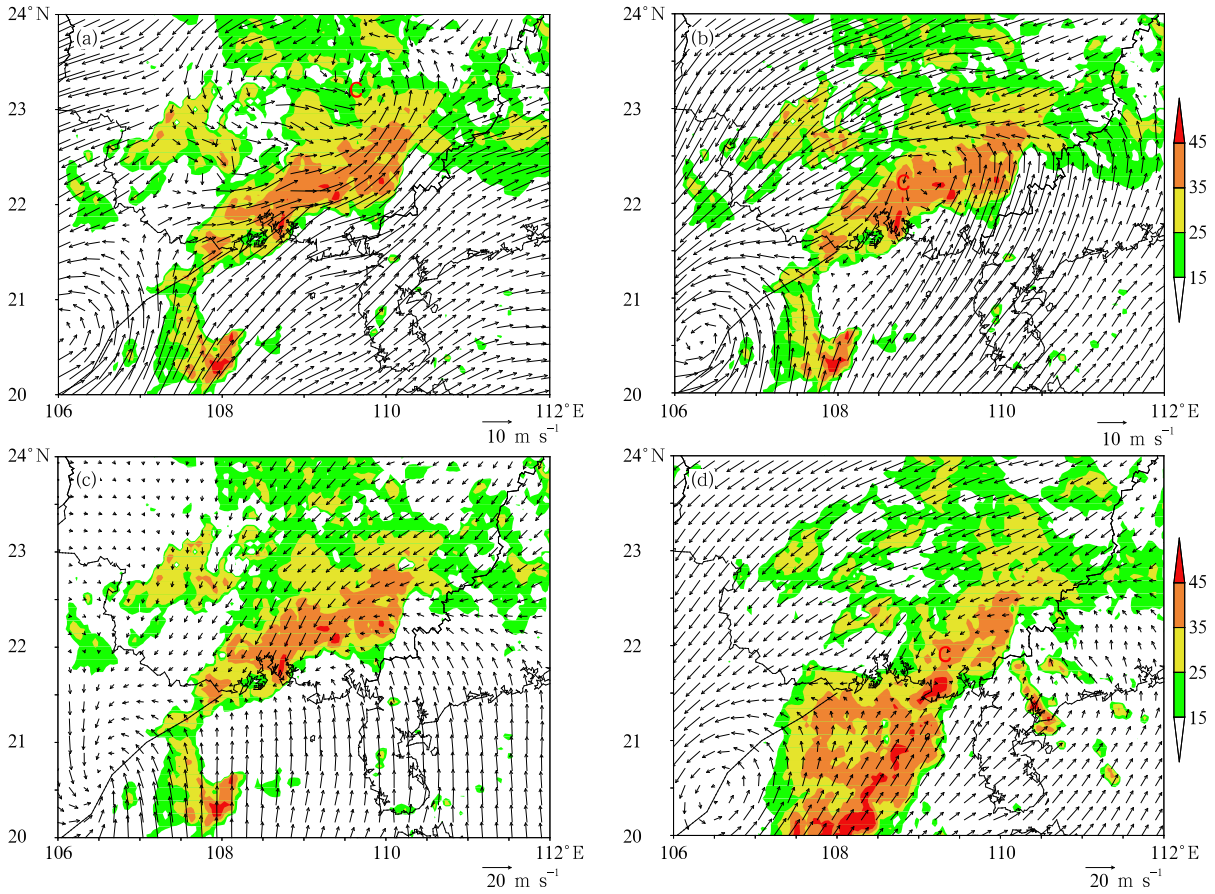

Fig. 3. SCHeREX wind field (vectors) and radar reflectivity (shadings) at (a) 700 hPa at 1800 UTC, (b) 850 hPa at 1800 UTC, (c) 925 hPa at 1800 UTC, and (d) 850 hPa at 2100 UTC 18 May 2008 over South China.

Delta on 10 June 2008. From 0000 UTC 10 June to 0000 UTC 11 June, the 24-h precipitation was 146 mm in Shaoxing. The flow field and radar reflectivity at 0900 UTC 10 June was shown in Fig. 4. At 700, 850, and 925 hPa of the SCHeREX mesoscale analysis, a meso-β-scale cyclone was generated in southern Anhui and Jiangsu. The cyclone at 700 hPa was slightly northward, while that at 850 and 925 hPa corresponded to the locations of two strong precipitation centers and the center of strong radar echo. In the geopotential height field at 850 hPa (Fig. 4d), two meso-β-scale low-pressure systems corresponded to the meso-β-scale cyclone. The generation and development of the mesoscale vortex coincided with that of the strong precipitation.

Comparisons between the SCHeREX analysis, radar echo and TBB of the heavy rainfall in Jianghuai on 21 June and that in South China from 2–3 June 2009 were respectively shown in Figs. 5 and 6. At 0600 UTC 21 June, an east-west shear line was distributed in southern Henan and central Anhui in the 850-hPa wind field. It was shown in Fig. 5 that three hours later, a meso-β-scale low-pressure vortex was generated in southern Henan, which corresponded to the high-value zone of radar echo, while the low value zone of TBB also expanded. This indicates that in the development stage, the evolution trend of the system was captured by the SCHeREX analysis. Six hours later, with eastward and southward shifting of the system, a mature vortex system was generated in the SCHeREX mesoscale wind field at the junction of Hubei, Henan, and Anhui provinces, which corresponded to the occurrence of strong local precipitation and was consistent with the high-value zone of radar echo and low-value center of TBB. Therefore, the SCHeREX mesoscale analysis performed well in

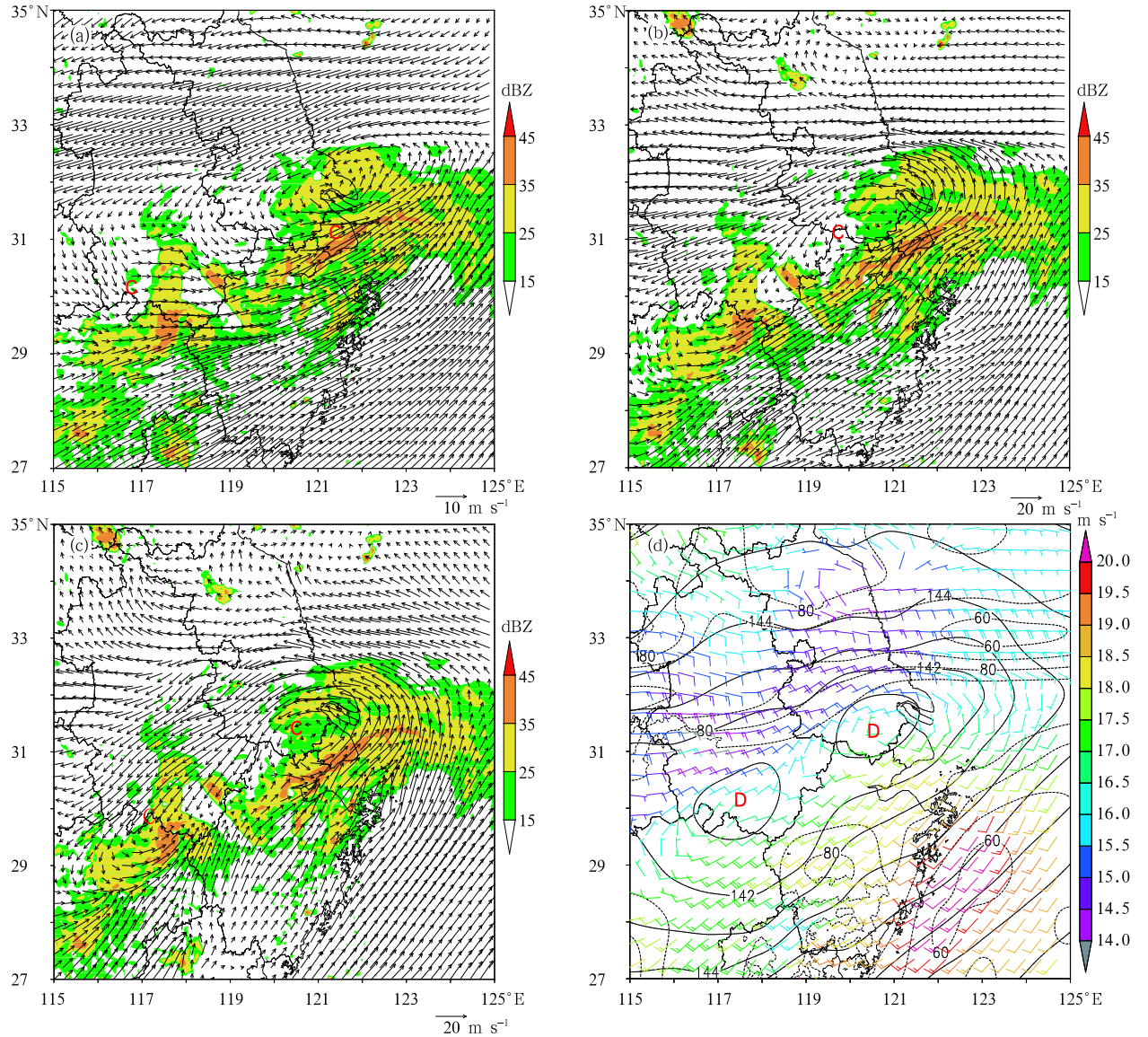

Fig. 4. SCHeREX wind field (vectors), radar reflectivity (shadings; dBZ) at (a) 700 hPa, (b) 850 hPa, and (c) 925 hPa; and (d) the geopotential height field (in 10 gpm) at 850 hPa in the Yangtze River Delta area at 0900 UTC 10 June 2008.

capturing the local heavy rainfall in Jianghuai area caused by the development and evolution of the meso-β-scale vortex.

Figure 6 shows that in the 850-hPa wind field at 1800 UTC 2 June, a vortex system occurred to the northwest of the rainfall area, which was consistent with the low-value zone of TBB and the strong radar echo. Three hours later, the system split and moved toward northeast with the meso-β-scale vortex to the north of the rainfall area, and convergence of wind field formed in the precipitation area; this corresponded to the low-value center of TBB and the strong radar echo. Six hours later, the system weakened, and the convergence of wind continued over the precipitation area with the rainfall location basically close to that at 2100 UTC; meanwhile, the corresponding low-value center of TBB shrank with reduced intensity; such temperature variations in the low-value center of TBB and radar echo were consistent with those in the SCHeREX mesoscale analysis field. Through the above analysis, it was proved that the SCHeREX mesoscale analysis was able to reproduce the development and evolution of the meso-β-scale systems in two precipitation events because the analysis results were consistent with the

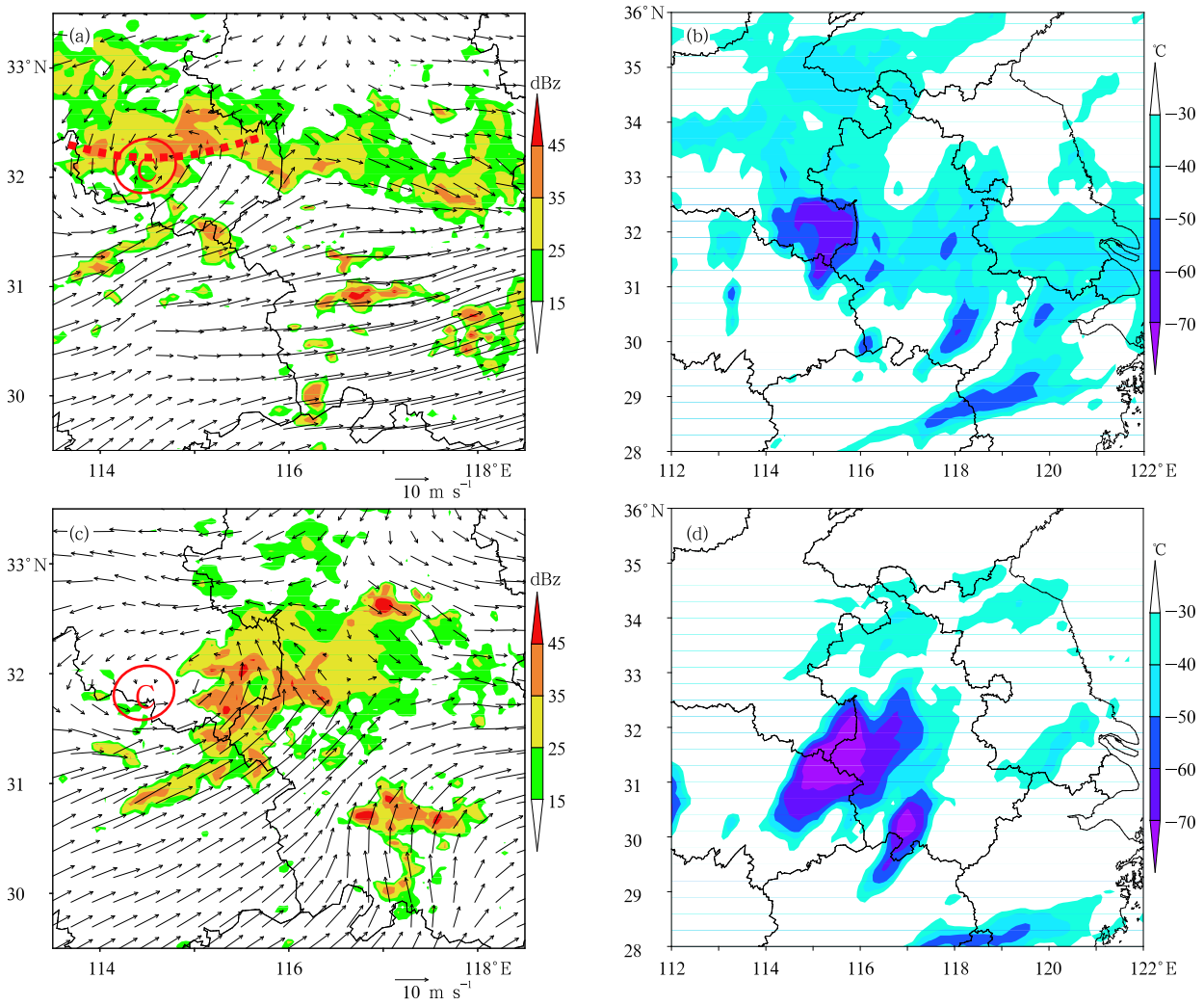

Fig. 5. SCHeREX wind vector field and radar reflectivity (dBZ; shadings; left panels), and TBB (°C; right panels) at 850 hPa in Jianghuai area at 0900 UTC (upper panels) and 1200 UTC (lower panels) 21 June 2008.

observations of radar and satellite.

5. Statistical evaluation of the SCHeREX mesoscale analysis data

5.1 Method

Quantitative verification of the SCHeREX analysis was carried out through the calculation of mean bias and root mean square error (RMSE) as follows

$$\mathrm{MB} = \frac{1}{N}\sum_{i=1}^{n}(x_i - x_\mathrm{o}), \tag{1}$$

$$\mathrm{RMSE} = \left[\frac{1}{N}\sum_{i=1}^{n}(x_i - x_\mathrm{o})^2\right]^{\frac{1}{2}}, \tag{2}$$

where x_i represents an analysis variable, x_o is the true value of observation, and N is the number of samples.

The SCHeREX was conducted from 0000 UTC 1 May to 1800 UTC 20 July 2008 and the same period in 2009. The acquired data included radiosonde data at 6-h intervals, Doppler radar data every 6 min, surface observation (automatic weather station) data, and so on. The comparison between the SCHeREX mesoscale analysis data and the radiosonde data was performed. First, the intensive radiosonde data obtained four times a day were hypothesized as true values (x_o), and the SCHEeREX mesoscale analysis gridded data interpolated onto 11 standard isobaric surfaces were considered as x_i. Equations (1) and (2) were used to derive the average deviation and RMSE

at each level in the four observation areas. The variables for statistical analysis included geopotential height, temperature, relative humidity, wind direction, and wind velocity.

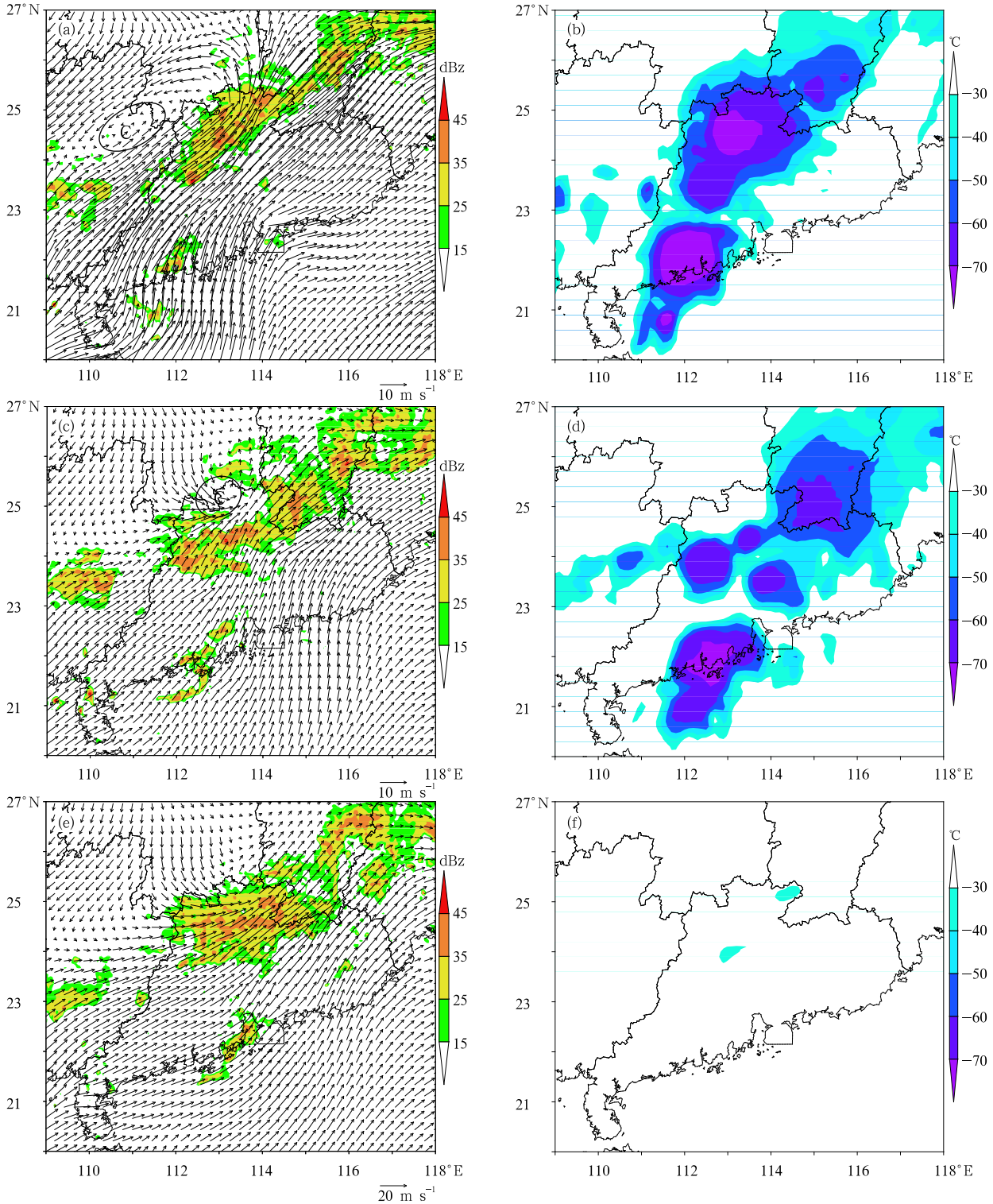

Fig. 6. SCHeREX wind vector field and radar reflectivity (dBZ; shadings; left panels), and TBB (°C; right panels) at 850 hPa in Jianghuai area at 1800 UTC 2 June 2008 (upper panels), 2100 UTC 2 June 2008 (middle panels), and 0000 UTC 3 June 2008 (lower panels).

5.2 Results

A three-dimensional average deviation is defined as the arithmetic mean of deviation values at all vertical levels and horizontal grids according to Eq. (1), hereinafter referred to as the "average deviation". As listed in Table 3, the average deviations of various meteorological variables were relatively small in the SCHeREX mesoscale analysis. In particular, the average deviations of geopotential height and wind fields were significantly small. In terms of regional distributions, the average deviation over Yangtze River Delta was slightly larger, but the maximum average deviation of relative humidity appeared in Central China, and those of various meteorological variables in other areas were roughly equal.

The magnitude of the average deviation was unable to reflect the true analysis precision of the SCHeREX mesoscale analysis data; it only revealed the systematic error of an analysis variable. Table 3 shows that the average deviations of geopotential height and wind fields were relatively small, so there were no significant systematic errors in these two variables. However, it is found that the SCHeREX mesoscale analysis data tended to overestimate relative humidity and wind direction and to underestimate temperature.

The RMSE listed in Table 4 can truly reflect the range of analytical errors. It can be clearly seen from Table 4 that the average RMSE of geopotential height, temperature, relative humidity, wind velocity, and wind direction were 44–45 gpm, 1.0–1.1°C, 35%, 2.5 m s^{-1}, and 24°–25°, respectively. The spatial distributions of RMSE also had obvious regional characteristics, and the RMSE of geopotential height was up to 85 gpm in Jianghuai area, while the minimum was only 15 gpm in Central China, and those of other two areas were about 50 gpm. The maximum RMSE of temperature was 1.4°C in Yangtze River Delta while the minimum was 0.8°C in South China, and those of the other two areas were 0.9 and 1.1°C, respectively. The average RMSE of relative humidity was roughly equal in the four observation areas with values ranging from 30% to 37%. The average RMSE of wind direction was rather consistent in the four areas with values of 2.0–2.5 m s^{-1}.

Table 3. Mean bias of each element in the four observation areas

	Meteorological variables				
	Height (gpm)	Temperature (°C)	Relative humidity (%)	Wind direction (°)	Wind velocity (m s^{-1})
South China	–5.009	0.022	22.683	6.39	–0.057
Central China	–5.099	0.029	18.541	8.818	–0.175
Jianghuai	–4.750	0.001	11.753	9.789	–0.145
Yangtze River	12.640	–1.778	–13.561	19.839	0.138
Average	–2.218	–1.726	9.854	11.209	–0.060

Table 4. RMSE of each element in the four observation areas

	Meteorological variables				
	Height (gpm)	Temperature (°C)	Relative humidity (%)	Wind direction (°)	Wind velocity (m s^{-1})
South China	54.535	0.762	36.893	18.154	1.922
Central China	15.374	0.879	35.589	22.235	1.395
Jianghuai	85.078	1.116	30.044	22.582	2.194
Yangtze River	21.542	1.376	35.800	34.583	4.404
Average	44.133	1.033	34.582	24.389	2.479

Figure 7 shows that the average deviation and RMSE of geopotential height, temperature, and humidity varied with height in Jianghuai area. The average deviation showed no significant variation with height while RMSE increased rapidly with height. The RMSE of geopotential height below 700 hPa was no more than 50 gpm while it changed downward to 25 gpm at 850 hPa and 12–13 gpm at 925 hPa, and upward to 125 gpm at 500 hPa and 175 gpm at 200 hPa. The RMSE of temperature below 700 hPa was less than 1.5–1.6°C; in particular, it was below 1°C in the lower troposphere except for 850 hPa. The RMSE of relative humidity below 700 hPa was less than 15%, and between 700 and 400 hPa it was less than 20%.

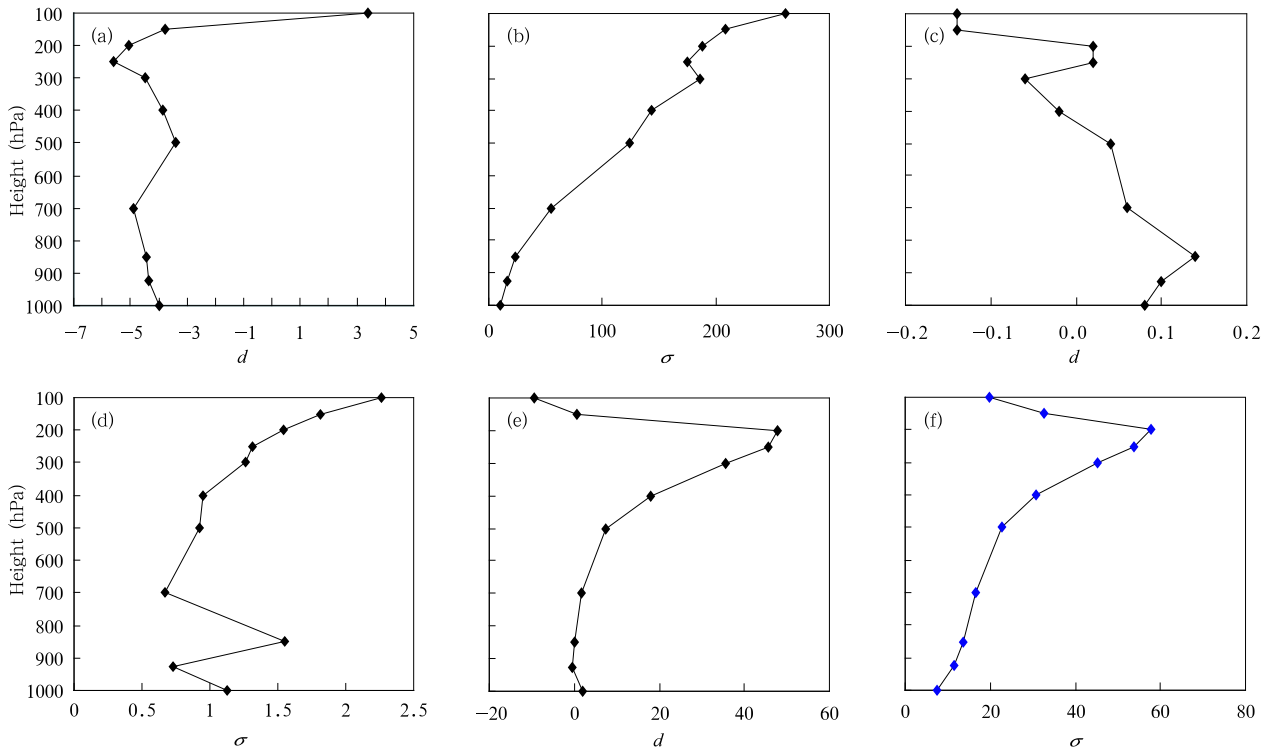

Fig. 7. Vertical distributions of mean error (a, c, e) and RMSE (b, d, f) of geopotential height (gpm; a, b), temperature (°C; c, d), and relative humidity (%; e, f) in Jianghuai area in 2008.

The large RMSE values of the above variables occurred above 400 hPa. Since severe mesoscale convective systems mainly resided at or below 700 hPa, and water vapor was also concentrated in the mid-low troposphere where the moisture flux convergence was most closely related to strong precipitation. It is thus inferred that the smaller the RMSEs of temperature, relative humidity and geopotential height at and below 700 hPa were, the stronger the capacity of the data in describing the characteristics of these mesoscale systems would be. In brief, the analytical error of geopotential height at or below 700 hPa was no less than 50 gpm, that of temperature was less than 1.6°C, and that of relatively humidity was less than 15%; so the analytical errors of the SCHeREX mesoscale analysis data were within the range of observation errors.

Vertical distributions of the average deviation and RMSE of wind direction and wind speed in Jianghuai area were shown in Fig. 8. It can be seen that the average deviation and RMSE of wind speed showed contrary variations with height compared to those of wind direction, i.e., small values existed in the lower troposphere and they increased with height. The RMSE of wind speed from 500 to 850 hPa was about 1.6 m s^{-1} while it was 1.8 m s^{-1} at 925 hPa. The low-level winds may be influenced by topography and underlying surface conditions, so the RMSE of wind direction decreased with height. Although the radar radial wind was assimilated by LAPS, perhaps due to the shelter of topography and urban high-rise buildings, the analysis precision of wind speed at low levels was not improved; instead, the RMSE of wind direction and wind speed both became larger at low levels. In summary, the analytical error of wind direction was 20°–30° at 700–925 hPa in the SCHeREX mesoscale analysis over the Jianghuai area, while that of wind speed below 500 hPa was no more than 1.6 m s^{-1} and reached 1.8 m s^{-1} at 925 hPa. As for mesoscale analysis, these errors were acceptable and within the range of observation errors.

Vertical distributions of the average deviation and RMSE of geopotential height, temperature and relative humidity in Yangtze River Delta were shown in Fig. 9. It is seen that the vertical distribution

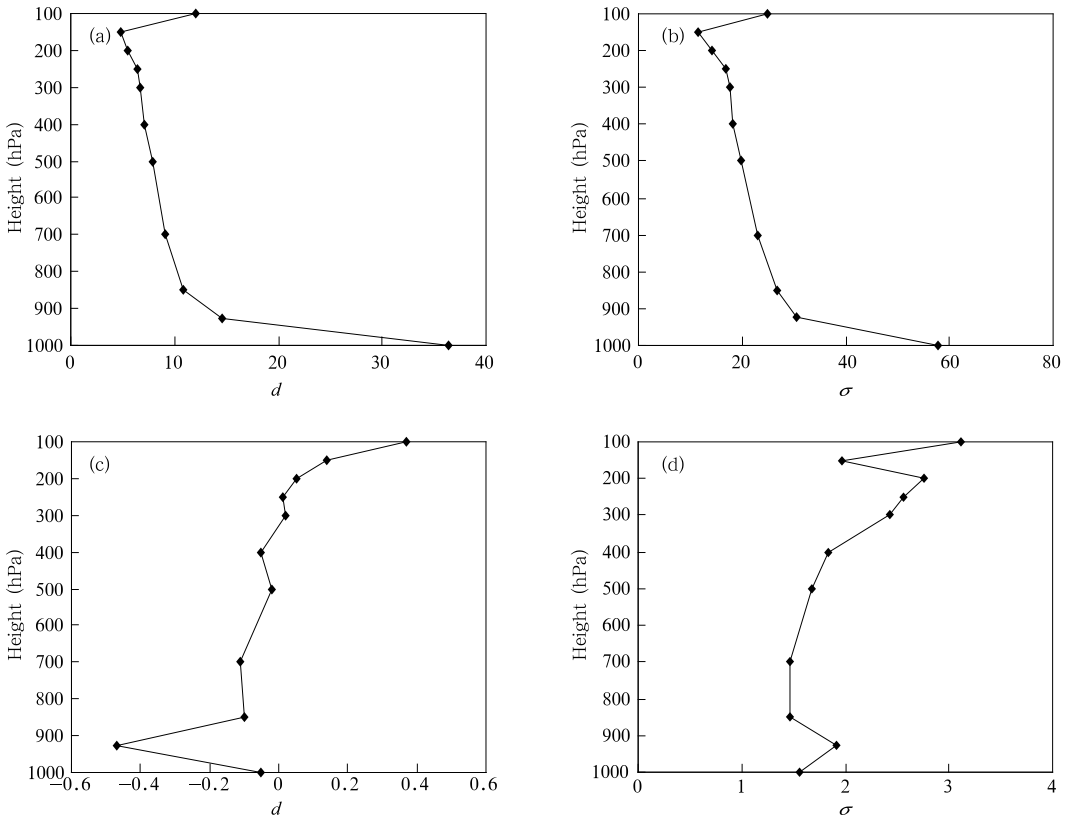

Fig. 8. Vertical distributions of mean bias (a, c) and RMSE (b, d) of wind direction (a, b) and wind speed (c, d) in Jianghuai area in 2008.

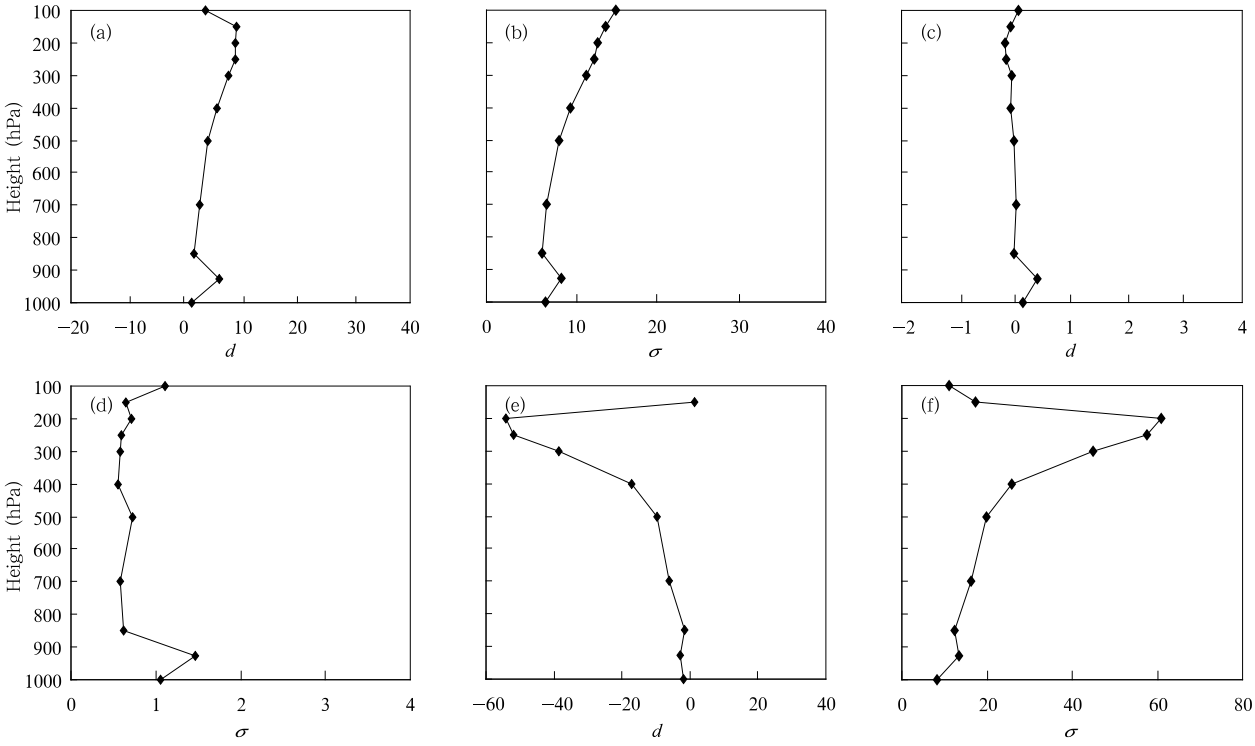

Fig. 9. As in Fig. 7, but for Yangtze River Delta in 2009.

characteristics of the above three variables were similar to those of Jianghuai area, while all the RMSEs at various heights over Yangtze River Delta were smaller than those over Jianghuai area. The RMSE of geopotential height below 500 hPa was < 20 gpm; that of temperature from the lower troposphere to 200 hPa < 0.6°C, and that of relative humidity below 500 hPa < 20%. The RMSEs of the above three variables in Yangtze River Delta were smaller than those in Jianghuai area. All the results were within the range of observation errors.

Figure 10 shows vertical distributions of the average deviation and RMSE of wind direction over Yangtze River Delta. The variations of the wind field were consistent with those over Jianghuai area. The RMSE of wind direction decreased with height while that of wind speed showed an opposite trend, which was significantly smaller than that in Jianghuai area. The RMSE of wind direction above 850 hPa was < 20°, and it reached 40° at 925 hPa. The RMSE of wind speed within 500–850 hPa was < 2.0 m s^{-1}, and it reached 3.5 m s^{-1} at 925 hPa. The larger RMSEs of wind direction and wind speed at 925 hPa were related to the influence of topography and underlying surface conditions. This was more obvious in Yangtze River Delta where more advanced urban construction and development occurred. The near-surface observation precision was influenced as the radar observation was sheltered by urban buildings and topography. However, such influences disappeared basically above 850 hPa with the analytical errors within the range of observation errors.

The vertical variations of RMSEs of geopotential height, temperature, relative humidity, wind direction, and wind speed in the SCHeREX mesoscale analysis fields of South China and Central China were similar to those in Jianghuai and Yangtze River Delta. No descriptions were repeated herein.

To sum up, the above analysis clearly showed that the average analytical error of geopotential height at 700–925 hPa in the SCHeREX mesoscale analysis data was about 45 gpm; that of temperature was 1.0–1.1°C; that of relative humidity was lower than 20%; that of wind velocity was 1.5–2.0 m s^{-1}, and that of wind

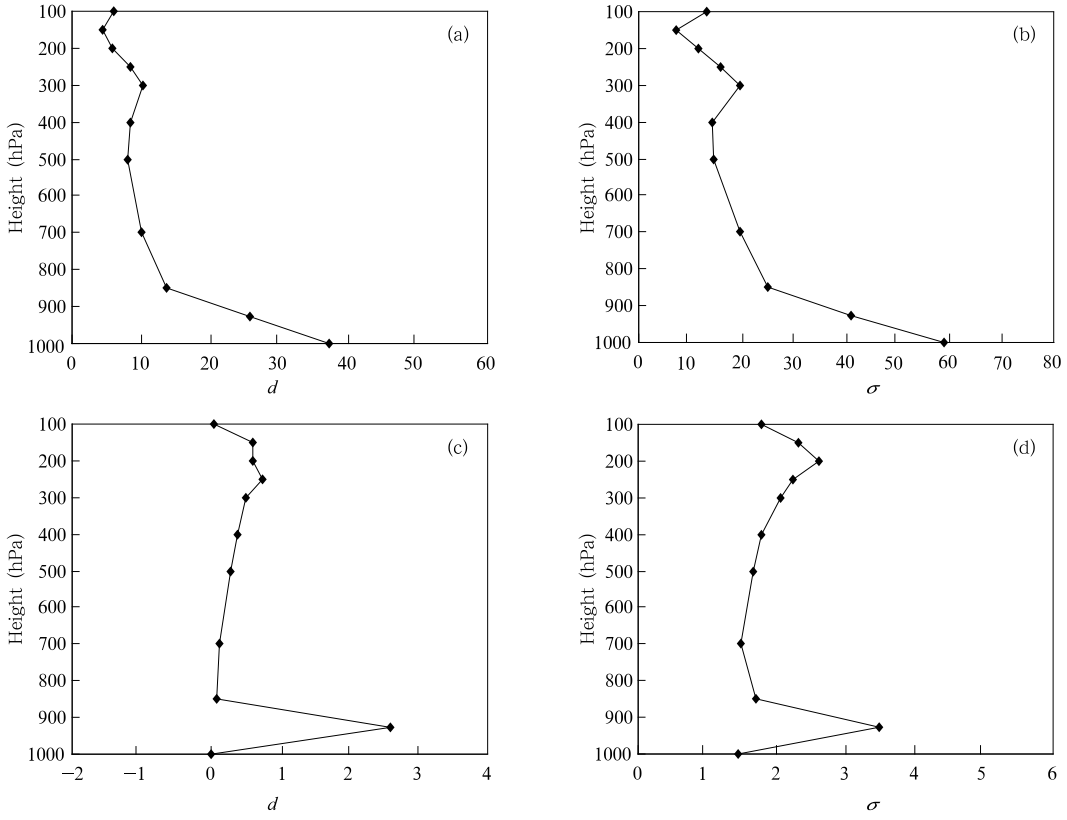

Fig. 10. As in Fig. 8, but for Yangtze River Delta in 2009.

direction was 20°–25°. The analytical errors of these variables increased with height (except for wind direction). Among the four observation areas, the analytical errors were greater in Jianghuai area. As for the mesoscale analysis, these results were acceptable and within the range of observation errors.

6. Conclusions and discussion

The LAPS system was used to integrate radiosonde, radar, upper air sounding, and surface observation data obtained in the South China Heavy Rainfall Experiment (SCHeREX) in four observation areas of South China, Central China, Jianghuai and Yangtze River Delta during 1 May–20 July 2008 and 2009. Accordingly, the SHCeREX mesoscale analysis data were generated with a horizontal resolution of 5 km and a temporal resolution of 3 h. An evaluation was carried out on the quality of the above data. First, the SCHeREX mesoscale analysis data were compared with the observation data of radar echo and TBB, and the capability of the SCHeREX mesoscale analysis in reproducing mesoscale convective systems associated with heavy rainfalls was analyzed. Then, in reference with radiosonde observations, vertical distributions of average deviation and RMSE of the SCHeREX mesoscale analysis were examined to reveal the analytical errors of the SCHeREX mesoscale analysis quantitatively. The following conclusions were drawn from the above analyses:

1) The SCHeREX mesoscale analysis generated by LAPS was able to capture 80% of the mesoscale (especially the meso-α-scale and meso-β-scale) weather systems inducing heavy rainfall. The dataset had a good capability in reproducing mesoscale systems; however, it was short of capacity in capturing smaller-scale systems such as the meso-γ-scale system. For the heavy rainfalls induced by the eastward moving meso-β-scale low-pressure vortex and shear line, the development and evolution of the mesoscale systems could be well reproduced by the SCHeREX mesoscale analysis.

2) The results from quantitative error evaluation of the SCHeREX mesoscale analysis show that the analytical errors in geopotential height, temperature, relative humidity, wind direction, and wind speed were within the range of observation errors. Specifically, the average analytical error of geopotential height at 700–925 hPa was 45 gpm; that of temperature was 1.0–1.1°C; that of relative humidity was smaller than 20%; that of wind velocity was 1.5–2.0 m s^{-1}, and that of wind direction was 20°–25°. The biases and RMSEs increased with height. It was inferred that the errors mainly stemmed from the mid-high troposphere while the main structural characteristics of mesoscale systems were reproduced at the mid-low levels of troposphere. Therefore, the increase of errors with height was supposed to have no significant influences on the mesoscale diagnosis and analysis using this dataset. Overall, the SCHeREX mesoscale analysis was applicable with high reliability.

Through the above analyses, it can be seen that there is still room for improvement in terms of the quality of the SCHeREX mesoscale analysis. The main task for next step is to use satellite data especially satellite radiation data in the LAPS analysis system sufficiently and effectively so as to improve the data quality at mid-high levels, and to further explore the potential of applying radar reflectivity in water vapor analysis in LAPS so as to raise the quality of moisture data. After these, the quality of the SCHeREX mesoscale analysis field is expected to improve significantly, and the data may be used as initial conditions for numerical weather models.

REFERENCES

Albers, S., J. McGinley, D. Birkenheuer, and J. Smart, 1996: The Local Analysis and Prediction System (LAPS): Analyses of clouds, precipitation, and temperature. *Wea. Forecasting*, **11**, 273–287.

Birkenheuer, D., 1999: The effect of using digital satellite imagery in the LAPS moisture analysis. *Wea. Forecasting*, **14**, 782–788.

——, 2000: Progress in applying GOES-derived data in local data assimilation. Preprints, 10th Conf. on Satellite Meteorology and Oceanography, Amer. Meteor. Soc., Long Beach, CA, 70–73.

Cui Chunguang, Li Hongli, Peng Juxiang, et al., 2009: The application of LAPS data to research a heavy rain event in East Hubei Province in the early sum-

mer of 2008. *Torrential Rain and Disasters*, **27**, 307–312. (in Chinese)

Hiemstra, C. A., G. E. Liston, R. A. Pielke, et al., 2006: Comparing Local Analysis and Prediction System (LAPS) assimilations with independent observations. *Wea. Forecasting*, **21**, 1024–1040.

Li Hongli, Cui Chunguang, and Wang Zhibin, 2009a: Scientific designs, functions and applications of LAPS. *Torrential Rain and Disasters*, **28**, 64–70. (in Chinese)

——, ——, ——, et al., 2009b: A study on application of Doppler radar data with LAPS. *Plateau Meteor.*, **28**, 1443–1452. (in Chinese)

——, Zhang Bing, and Chen Bo, 2008: Local Analysis and Prediction System (LAPS) and its localization. *Meteor. Sci. Technol.*, **36**, 20–24. (in Chinese)

McGinley, J. A., S. Albers, and P. Stamus, 1991: Validation of a composite convective index as defined by a real-time local analysis system. *Wea. Forecasting*, **6**, 337–356.

Ni Yunqi, Zhou Xiuji, Zhang Renhe, et al., 2006: Experiments and studies of heavy rainfall in southern China. *J. Appl. Meteor. Sci.*, **17**, 690–704. (in Chinese)

Snook, J. S., 1996: Local domain forecasting support to the 1996 Atlanta Olympic Games. Preprints, 12th Intl. Conf. on Interactive and Processing Systems for Meteorology, Oceanography, and Hydrology, Atlanta, GA, Amer. Meteor. Soc., 32–35.

——, P. A. Stamus, J. Edwards, Z. Christidis, and J. A. McGlinley, 1998: Local-domain mesoscale analysis and forecast model support for the 1996 Summer Olympic Games. *Wea. Forecasting*, **13**, 138–150.

Tao Shiyan, 1980: *Heavy Rainfall of China*. Science Press of China, 225 pp. (in Chinese)